Journal of Alloys and Compounds 509 (2011) L7–L10

Contents lists available at ScienceDirect

Journal of Alloys and Compounds

journal homepage: www.elsevier.com/locate/jallcom

Letter

Mechanical synthesis and rapid consolidation of a nanocrystalline $3.3Fe_{0.6}Cr_{0.3}Al_{0.1}$–$Al_2O_3$ composite by high frequency induction heating

In-Jin Shon[a,b,*], Tae-Wan Kim[a], Jung-Mann Doh[c], Jin-Kook Yoon[c], Sang-Whan Park[c], In-Yong Ko[a]

[a] Division of Advanced Materials Engineering and Research Center of Advanced Materials Development, Engineering College, Chonbuk National University, Chonbuk 561-756, Republic of Korea
[b] Department of Hydrogen and Fuel Cells Engineering, Specialized Graduate School, Chonbuk National University, Chonbuk 561-756, Republic of Korea
[c] Advanced Functional Materials Research Center, Korea Institute of Science and Technology, PO Box 131, Cheongryang, Seoul 130-650, Republic of Korea

ARTICLE INFO

Article history:
Received 1 August 2010
Accepted 14 September 2010
Available online 22 September 2010

Keywords:
Nanostructured materials
Sintering
Mechanical alloying
Mechanical properties
Composite materials

ABSTRACT

Nanopowders of $3.3Fe_{0.6}Cr_{0.3}Al_{0.1}$ and Al_2O_3 were synthesized from Fe_2O_3, Cr, and Al powders by high-energy ball milling. A high density nanocrystalline $3.3Fe_{0.6}Cr_{0.3}Al_{0.1}$–$Al_2O_3$ composite was consolidated by a high frequency induction heated sintering (HFIHS) method within 3 min from mechanically synthesized powders of Al_2O_3 and $3.3Fe_{0.6}Cr_{0.3}Al_{0.1}$. The average grain sizes of Al_2O_3 and $3.3Fe_{0.6}Cr_{0.3}Al_{0.1}$ were 84 and 32 nm, respectively.

1. Introduction

Iron–aluminum–chromium alloys are applicable as structural materials and coatings for high temperature applications [1]. Their excellent corrosion resistance is due to the formation of a dense, protective alumina scale. Alumina, α-Al_2O_3 in particular, demonstrates a low rate constant even at temperatures above 1,000 °C [2]. However, as with many alloys, $Fe_{0.6}Cr_{0.3}Al_{0.1}$ exhibits a low frictional resistance due to its low hardness. One method to improve hardness is to add Al_2O_3 to form composite nanostructured materials [3]. Traditionally, discontinuously reinforced metal matrix composites have been produced by several processes including powder metallurgy, spray deposition, mechanical alloying, casting, and self-propagating high temperature synthesis (SHS). A technique using high-energy ball milling and mechanical alloying of powder mixtures, which is a combination of mechanical milling and chemical reactions, has been reported to be efficient for the preparation of nanocrystalline metals and alloys [4].

Nanocrystalline materials have received much attention as advanced engineering materials due to their improved physical and mechanical properties [5,6]. Nanomaterials typically possess high strength, high hardness, excellent ductility, and toughness. Therefore, increasing attention has been paid to developing potential nanomaterial applications [7]. The grain sizes in sintered materials are much larger than in the pre-sintered powders due to the fast grain growth that occurs during conventional sintering processes. Therefore, controlling grain growth during sintering is one of the keys to the commercial success of nanostructured materials. High frequency induction-activated sintering methods, which can be used to quickly manufacture dense materials within 2 min, can be effective to control grain growth [8,9].

The goals of this work were to fabricate a new nanopowder using high-energy ball milling and a dense nanocrystalline Al_2O_3-reinforced Fe–Cr–Al composite within 3 min from mechanically alloyed powders via a high frequency induction activated sintering method and to evaluate its mechanical properties (hardness and fracture toughness) and grain size.

2. Experimental procedures

Powders of 99% pure Fe_2O_3 (<5 μm, Alfa Co.), 99.5% pure Al (<325 mesh, Alfa Co.), and 99.8% pure Cr (<10 μm, Alfa Co.) were used as the starting materials. Fe_2O_3, Cr, and 2.1Al powder mixtures were first milled in a high-energy ball mill (Pulverisette 5 planetary mill) at 250 rpm for 10 h. Tungsten carbide balls (8.5 mm in diameter) were used in a sealed cylindrical stainless steel vial under an argon atmosphere. The weight ratio of the balls-to-powder was 30:1. Milling resulted in a significant reduction of grain size. The grain sizes of the Fe–Cr–Al alloy and Al_2O_3 were calculated

* Corresponding author at: Division of Advanced Materials Engineering, Engineering College, Chonbuk National University, Deckjin-dong 1-ga, Duckjin-gu, Jeonju, Jeonbuk 561-756, Republic of Korea. Tel.: +82 63 2381; fax: +82 63 270 2386.
E-mail address: ijshon@chonbuk.ac.kr (I.-J. Shon).

0925-8388/$ – see front matter © 2010 Elsevier B.V. All rights reserved.
doi:10.1016/j.jallcom.2010.09.067

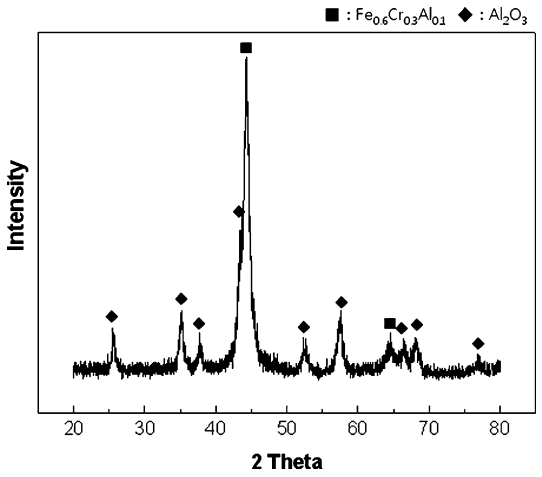

Fig. 1. XRD pattern of the mechanically alloyed $3Fe_{0.67}Cr_{0.33}$–Al_2O_3 powder.

using Suryanarayana's and Norton's formula [10]:

$$B_r(B_{\text{crystalline}} + B_{\text{strain}})\cos q = \frac{k\lambda}{L} + \sin q \quad (1)$$

where B_r is the full width at half-maximum (FWHM) of the diffraction peak after instrument correction, $B_{\text{crystalline}}$ and B_{strain} are the FWHM values caused by the small grain size and internal stress, respectively, k is a constant with a value of 0.9, λ is the wavelength of the X-ray radiation, L is the grain size, η is the internal strain, and θ is the Bragg angle. The parameters B and B_r follow Cauchy's form with the relationship $B = B_r + B_s$, where B and B_s are the FWHM values of the broadened Bragg peaks and the standard sample's Bragg peaks, respectively.

After milling, the mixed powders were placed in a graphite die (outside diameter of 45 mm, inside diameter of 20 mm, height of 40 mm) and then introduced into a pulsed current activated sintering system (Eltek, South Korea), which is shown schematically in [8,9]. The four major stages in the synthesis are: (Stage 1) evacuation of the system, (Stage 2) application of uniaxial pressure, (Stage 3) heating of the sample by an induced current, and (Stage 4) cooling of the sample. The process was carried out under a vacuum of 40 mTorr.

Microstructural information was obtained from product samples that were polished at room temperature. Compositional and microstructural analyses of the products were conducted using X-ray diffraction (XRD) and a scanning electron microscope (SEM) with energy dispersive X-ray analysis (EDAX). The Vickers hardness was measured by performing indentations on the sintered samples at a load of 50 kg and a dwell time of 15 s.

3. Results and discussion

The X-ray diffraction results for the high-energy ball milled powders are shown in Fig. 1. The Fe_2O_3, Cr, and Al reactant powders of were not detected whereas the products, Fe–Cr–Al alloy and Al_2O_3, were detected. Based on the above results, the mechanical alloy was completely formed during the milling. The net reaction can be considered as a combination of the following two reactions:

$$Fe_2O_3 + 2Al \rightarrow 2Fe + Al_2O_3 \quad (2)$$

$$2Fe + Cr + 0.1Al \rightarrow 3.3Fe_{0.6}Cr_{0.3}Al_{0.1} \quad (3)$$

Reaction (2) is the well known exothermic reaction for which the standard enthalpy of reaction ranges from −847 to −811 kJ over the temperature range of 700 °C (just above the melting temperature of Al, 660 °C) to 1,500 °C (just below the melting point of Fe, 1,536 °C).

The FWHM value obtained from the XRD pattern of the milled powder is larger than that of the raw powder due to internal strain and reduction of the grain size. Fig. 2 shows a plot of $B_r \sin\theta$ as a function of $\cos\theta$. The intercept ($K\lambda/L$) can be used to calculate the crystallite size (L). The average grain sizes of Fe–Cr–Al and Al_2O_3 determined by Suryanarayana's and Norton's formula were about 10 and 66 nm, respectively.

The variations in the shrinkage displacement and surface temperature of the graphite die with heating time during the processing of the Fe–Cr–Al and Al_2O_3 system are shown in Fig. 3. When an

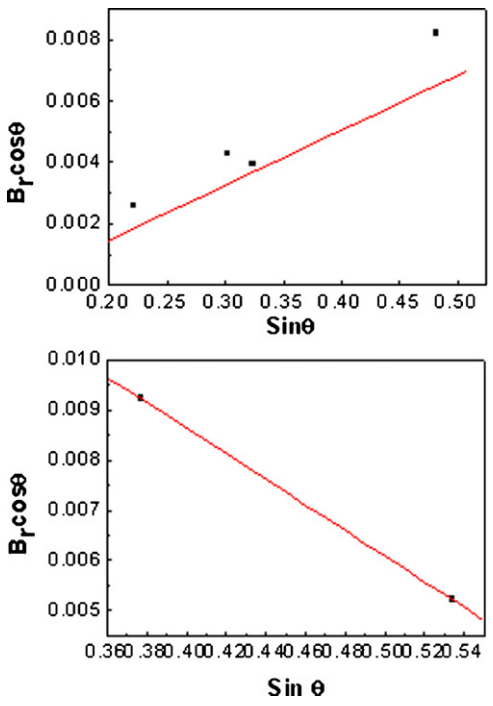

Fig. 2. Plot of $B_r \cos\theta$ versus $\cos\theta$ of $Fe_{0.67}Cr_{0.33}$ and Al_2O_3 in the mechanically alloyed powders.

induced current was applied, the specimen experienced thermal expansion and the shrinkage displacement slowly increased with temperature up to about 900 °C and then abruptly increased at about 1,150 °C. The X-ray diffraction pattern of a sample heated to 1,150 °C is shown in Fig. 4, where the Fe–Cr–Al alloy and Al_2O_3 were detected. Fig. 5 shows a plot of $B_r \cos\theta$ versus $\sin\theta$ used to calculate the structure parameters including the average grain sizes of the Fe–Cr–Al alloy and Al_2O_3. The grain sizes of the Fe–Cr–Al alloy and Al_2O_3 obtained from the X-ray data and using Suryanarayana's and Norton's formula were 32 and 84 nm, respectively. An

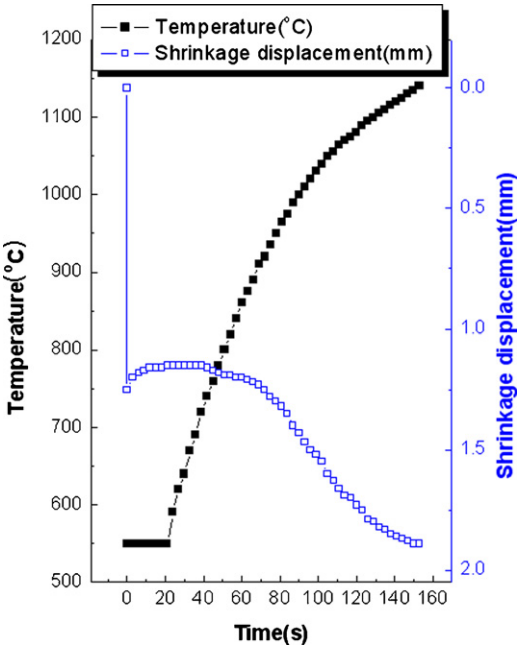

Fig. 3. Variations of the temperature and shrinkage displacement with heating time during high frequency induction heated sintering of $3Fe_{0.67}Cr_{0.33}$–Al_2O_3 powders.

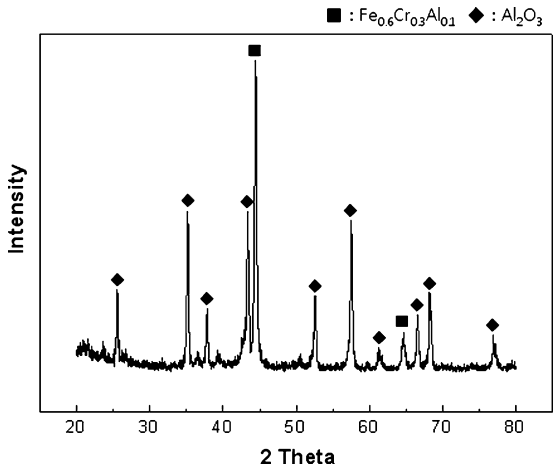

Fig. 4. XRD patterns of the $3Fe_{0.67}Cr_{0.33}$–Al_2O_3 composite heated to 1,150 °C.

FE-SEM image of the $3.3Fe_{0.6}Cr_{0.3}Al_{0.1}$–$Al_2O_3$ composite is shown in Fig. 6(a). It can be seen that the structure consisted of nanophases. The average grain sizes of the sintered Fe–Cr–Al alloy and Al_2O_3 are not significantly larger than the initial powders, indicating the absence of significant grain growth during sintering. This retention of the grain size is attributed to the high heating rate and the relatively short exposure of the powders to the high temperature. The role of the current (resistive or inductive) in sintering and or synthesis has been the focus of several attempts aimed at providing an explanation for the observed enhancement of sintering and the improved characteristics of the products. The role played by the current has been interpreted differently with the effect being explained in terms of the fast heating rate due to Joule heating, the presence of plasma in pores separating powder particles [11], and the intrinsic contribution of the current to mass transport [12–14].

Vickers hardness measurements were made on polished sections of the $3Fe_{0.67}Cr_{0.33}$–Al_2O_3 composite using a 50 kg_f load and a 15 s dwell time. The calculated hardness value of the

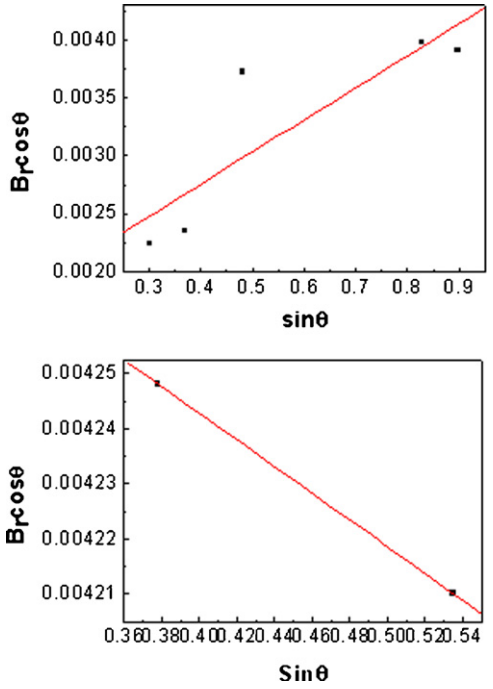

Fig. 5. Plot of $B_r \cos\theta$ versus $\cos\theta$ of $Fe_{0.67}Cr_{0.33}$ and Al_2O_3 in the composite sintered at 1,150 °C.

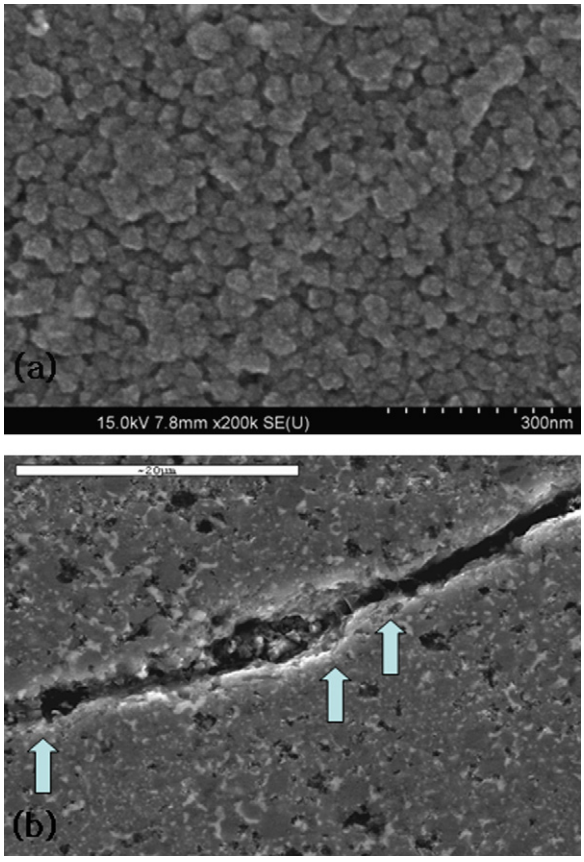

Fig. 6. (a) FE-SEM image and (b) median crack propagating of the $3Fe_{0.67}Cr_{0.33}$–Al_2O_3 composite heated to 1,150 °C.

$3Fe_{0.67}Cr_{0.33}$–Al_2O_3 composite was 1,160 kg/mm^2. This value represents an average of five measurements. Indentations with sufficiently large loads produced median cracks around the indent. The length of these cracks permits an estimation of the fracture toughness of the material using Niihara et al.'s expression [15]:

$$K_{IC} = 0.023\left(\frac{c}{a}\right)^{-3/2} H_v\, a^{1/2} \quad (4)$$

where c is the trace length of the crack measured from the center of the indentation, a is half of the average length of two indent diagonals, and H_v is the hardness.

The calculated fracture toughness value of the $3.3Fe_{0.6}Cr_{0.3}Al_{0.1}$–$Al_2O_3$ composite was about 15 MPa $m^{1/2}$. As in the case of the hardness value, the toughness value is the average of five measurements. A higher magnification view of the indentation median crack in the composite is shown in Fig. 6(b), which shows that the crack propagated deflectly (↑). The absence of reported hardness and toughness values of the $3.3Fe_{0.6}Cr_{0.3}Al_{0.1}$–$Al_2O_3$ composite precludes making direct comparisons to the results obtained in this study. However, the hardness and fracture toughnesses of Al_2O_3 with a grain size of 4.5 μm were previously reported as 1,800 kg/mm^2 and 4 MPa $m^{1/2}$, respectively [16]. The hardness of the $3.3Fe_{0.6}Cr_{0.3}Al_{0.1}$–$Al_2O_3$ composite is lower than that of monolithic Al_2O_3, but the fracture toughness is higher than the value of Al_2O_3 due to addition of the ductile Fe–Cr–Al alloy.

4. Conclusions

Nanopowders of Fe–Cr–Al and Al_2O_3 were fabricated from Fe_2O_3, Cr, and Al powders by high-energy ball milling. The average grain sizes of the Fe–Cr–Al alloy and Al_2O_3 prepared by HEBM were 10 and 66 nm, respectively. Using the high frequency induction activated sintering method, we accomplished densification of nanostructured $3.3Fe_{0.6}Cr_{0.3}Al_{0.1}$–$Al_2O_3$ composite from mechanically alloyed powders. Complete densification could be achieved within a processing time of 3 min under an applied pressure of 80 MPa and an induced current. The average grain sizes of the Fe–Cr–Al alloy and Al_2O_3 prepared by HFIHS were about 32 and 84 nm, respectively. The average obtained hardness and fracture toughness values were 1,160 kg/mm^2 and 15 MPa m$^{1/2}$, respectively.

Acknowledgement

This work was supported by the New & Renewable Energy R&D Program (2009T00100316) of the Ministry of Knowledge Economy, Republic of Korea.

References

[1] J. Klower, Mater. Corros. 47 (1996) 685–694.
[2] P. Kofstad, High Temperature Corrosion, Elsevier Appl. Sci. Publ., London/New York, 1988.
[3] N.R. Park, I.Y. Ko, J.M. Doh, W.Y. Kong, J.K. Yoon, I.J. Shon, Mater. Charact. 61 (2010) 277–282.
[4] S. Paris, E. Gaffet, F. Bernard, Z.A. Munir, Scripta Mater. 50 (2004) 691–696.
[5] M.S. El-Eskandarany, J. Alloys Compd. 305 (2000) 225–238.
[6] L. Fu, L.H. Cao, Y.S. Fan, Scripta Mater. 44 (2001) 1061–1068.
[7] S. Berger, R. Porat, R. Rosen, Prog. Mater. Sci. 42 (1997) 311–320.
[8] H.C. Kim, I.J. Shon, I.J. Jeong, I.Y. Ko, J.K. Yoon, J.M. Doh, Met. Mater. Int. 13 (2007) 39–46.
[9] H.C. Kim, I.J. Shon, I.K. Jeong, I.Y. Ko, Met. Mater. Int. 12 (2006) 393–399.
[10] C. Suryanarayana, M. Grant Norton, X-ray Diffraction A Practical Approach, Plenum Press, 1998, p. 213.
[11] Z. Shen, M. Johnsson, Z. Zhao, M. Nygren, J. Am. Ceram. Soc. 85 (2002) 1921–1927.
[12] J.E. Garay, U. Anselmi-Tamburini, Z.A. Munir, S.C. Glade, P. Asoka-Kumar, Appl. Phys. Lett. 85 (2004) 573–575.
[13] J.R. Friedman, J.E. Garay, U. Anselmi-Tamburini, Z.A. Munir, Intermetallics 12 (2004) 589–597.
[14] J.E. Garay, U. Anselmi-Tamburini, Z.A. Munir, Acta. Mater. 51 (2003) 4487–4495.
[15] K. Niihara, R. Morena, D.P.H. Hasselman, J. Mater. Sci. Lett. 1 (1982) 12–16.
[16] M.N. Rahaman, A. Yao, B. Sonny Bal, J.P. Garino, M.D. Ries, J. Am. Ceram. Soc. 90 (2007) 1965–1988.